ELSEVIER

Biochimica et Biophysica Acta 1461 (1999) 113–122

BIOCHIMICA ET BIOPHYSICA ACTA
BBA

www.elsevier.com/locate/bba

The ion-channel activity of longibrachins LGA I and LGB II: effects of Pro-2/Ala and Gln-18/Glu substitutions on the alamethicin voltage-gated membrane channels

Pascal Cosette [a], Sylvie Rebuffat [b], Bernard Bodo [b], Gérard Molle [a,*]

[a] *UMR 6522 CNRS, Université de Rouen (IFRMP 23–GDR 790 CNRS), Boulevard M. de Broglie, 76821 Mont-Saint-Aignan, France*
[b] *Laboratoire de Chimie des Substances Naturelles, ESA 8041 CNRS, GDR 790 CNRS, IFR 63 CNRS-INSERM, Muséum National d'Histoire Naturelle, 63 rue Buffon, 75231 Paris Cedex 05, France*

Received 21 April 1999; received in revised form 31 August 1999; accepted 7 September 1999

Abstract

Longibrachins LGA I (Ac Aib Ala Aib Ala Aib[5] Ala Gln Aib Val Aib[10] Gly Leu Aib Pro Val[15] Aib Aib Gln Gln Pheol[20], with Aib: α-aminoisobutyric acid, pheol: phenylalaninol) and LGB II are two homologous 20-residue long-sequence peptaibols isolated from the fungus *Trichoderma longibrachiatum* that differ between them by a Gln-18/Glu substitution. They distinguish from alamethicin by a Pro-2 for Ala replacement, which allowed to examine for the first time with natural Aib-containing analogues, the effect of Pro-2 on the ion-channel properties exhibited by alamethicin. The influence of these structural modifications on the voltage-gated ion-channel forming activity of the peptides in planar lipid bilayers were analysed. The general 'barrel-stave' model of ion-channel activity, already described for alamethicin, was preserved with both longibrachins. The negatively charged LGB II promoted higher oligomerisation levels, which could presumably dilute the repulsive effect of the negative Glu ring near the entrance of the channel and resulted in lower lifetimes of the substates, confirming the strong anchor of the peptide C-terminus at the *cis*-interface. Reduction of the channel lifetimes was observed for the longibrachins, compared to alamethicin. This argues for a better stabilisation of the channels formed by peptaibols having a proline at position 2, which results in better anchoring of the peptide monomer N-terminus at the *trans*-bilayer interface. Qualitative assays of the temperature dependence on the neutral longibrachin channel properties demonstrated a high increase of channel lifetimes and a markedly reduced voltage-sensitivity when the temperature was decreased, showing that such conditions may allow to study the channel-forming properties of peptides leading to fast current fluctuations.

Keywords: Alamethicin; Longibrachin; Peptaibol; Transmembrane peptide; Planar lipid bilayer; Macroscopic current; Single-channel recording; Temperature

1. Introduction

Longibrachins are natural peptides belonging to the peptaibol class of antibiotics, which were isolated from the fungus *Trichoderma longibrachiatum*. Peptaibols are linear peptides characterised by an acetylated N-terminus, a high proportion of α-amino-isobutyric acid (Aib) and a C-terminal amino alcohol. The most largely represented peptaibols contain 18–20 residues. They are qualified as long-sequence pep-

* Corresponding author. Fax: +33-2-3514-6704; E-mail: gerard.molle@univ-rouen.fr

0005-2736/99/$ – see front matter
PII: S0005-2736(99)00153-4

taibols and are exemplified by alamethicin (Alm), the first isolated and widely studied peptaibol [1–3]. The sequences of longibrachins LGA I and LGB II, two homologous peptaibols isolated from the natural longibrachin mixture, are highly similar to those of the neutral (Alm F50; Gln-18) and acidic (Alm F30 I; Glu-18) alamethicins, respectively [1–3], the only difference being a Pro-2/Ala substitution (Table 1). It is now well admitted that long-sequence peptaibols adopt a largely predominant α-helical conformation [4,5] resulting from the high proportion of Aib in the peptides. This structuration, together with the high mean hydrophobicity of the primary structure, gives them a potent ability for translocation into membrane bilayers that they strongly permeabilise in the absence of voltage [6–9]. In the presence of voltage, they auto-associate in lipid bilayers and form ion channels with specific characteristics [9–11]. This membrane activity has been shown to result in the antibiotic properties of peptaibols and particularly in the antimycoplasmic properties [9,12].

After incorporation of Alm into lipid bilayers, ionic current measurements demonstrate a channel-forming activity, in agreement with the 'barrel-stave' model [13,14] which is characterised by a change in channel size caused by uptake and release of peptide monomers in the conducting helix bundles. Among the amino acids which could be critical for the ion-channel activity, the two prolines occurring in the Alm sequence at positions 2 and 14 could be of particular interest, as this residue has been reported to play a role in transmembrane segments and to affect the helix bending and stability, due to the lack of amide proton that could be involved in the hydrogen bonding scheme [15,16]. In the case of long-sequence peptaibols, such as Alm or trichorzianins, the proline close to the centre of the peptide has been shown to create a flexible hinge [17,18] proposed to play a major role in the voltage-gated formation of the channels [4,17,18]. In order to estimate the influence of both prolines and, as no natural analogues with such typical substitutions at the proline positions were available, synthetic analogues in which all Aib residues have been replaced by leucines (des-Aib-Leu analogues, diBL) were prepared and investigated [19]. When incorporated in planar lipid bilayers, the diBLP2A (Pro-2/Ala replacement) and diBL-P14A (Pro-14/Ala replacement) analogues (Table 1) still exhibited a voltage-dependent activity, but produced very fast alamethicin-like fluctuations, indicating changes in the channel stability. Both proline substitutions reduced the mean dwell-time, with a more pronounced effect for the Pro-14 substitution. Recently, the replacement of Pro-14 for Ala was carried out in the sequence of Alm [20]. The ion-channel properties of the resulting synthetic Aib-peptide confirmed the role previously proposed for Pro-14 [19]. However, the effect of Pro-2 was not investigated by using such synthetic peptides. Although several natural 20-residue peptaibols without such a Pro-2 have been studied as regard their ion-channel forming properties [7,21], the corresponding sequences exhibited, in all cases, several other amino acid substitutions compared to the sequence of Alm (Table 1), which prevented to examine unambiguously the role of this single residue.

The sequences of longibrachins LGA I and LGB II only differ by a Pro-2/Ala substitution from those of Alm F50 and Alm F30 I, respectively. They thus appeared as excellent candidates for examining for the first time the role of a proline at position 2 with natural Aib-containing analogues. In addition,

Table 1
Sequences of selected 20-residue natural peptaibols: longibrachins LGA I and LGB II, alamethicin F50 (Alm F50) and F30 I (Alm F30 I) [3], trichocellins TCA II and TCB II [21], saturnisporin SA IV [7], trichosporin TSB VIa [30] and of the synthetic des-Aib-Leu analogues of alamethicin: diBL, diBLP2A and diBLP14A [19]

	1				5					10					15					20
LGA I	AcU	A	U	A	U	A	Q	U	V	U	G	L	U	P	V	U	U	Q	Q	Fol
LGB II	AcU	A	U	A	U	A	Q	U	V	U	G	L	U	P	V	U	U	E	Q	Fol
Alm F50	AcU	P	U	A	U	A	Q	U	V	U	G	L	U	P	V	U	U	Q	Q	Fol
Alm F30I	AcU	P	U	A	U	A	Q	U	V	U	G	L	U	P	V	U	U	E	Q	Fol
TCA II	AcU	A	U	A	U	A	Q	U	L	U	G	U	U	P	V	U	J	Q	Q	Fol
TCB II	AcU	A	U	A	U	A	Q	U	L	U	G	U	U	P	V	U	J	E	Q	Fol
SA IV	AcU	A	U	A	U	U	Q	U	L	U	G	U	U	P	V	U	J	Q	Q	Fol
TSB VIa	AcU	A	U	A	U	U	Q	U	I	U	G	L	U	P	V	U	U	Q	Q	Fol
diBL	AcL	P	L	A	L	A	Q	L	V	L	G	L	L	P	V	L	L	E	Q	Fol
diBLP2A	AcL	A	L	A	L	A	Q	L	V	L	G	L	L	P	V	L	L	E	Q	Fol
DiBLP14A	AcL	P	L	A	L	A	Q	L	V	L	G	L	L	A	V	L	L	E	Q	Fol

U codes for Aib: α-amino-isobutyric acid, J for Iva: isovaline and Fol for pheol: phenylalaninol.

the Gln-18/Glu substitution occurring in the couple of peptaibols LGA I/LGB II could allow to re-evaluate the effect of a negative charge in the peptide C-terminus and to compare the results with those previously obtained with neutral and charged pairs of such related peptaibols [22,23]. We thus report here the characterisation of the longibrachin LGA I and LGB II ion-channel forming properties. In order to allow easier comparison of the data with those available in the literature, two different lipid compositions (POPC/DOPE (7:3) and DPhPC) were used in the study. Finally, the role of the temperature on the single-channel stability was analysed for the neutral longibrachin LGA I.

2. Materials and methods

2.1. Isolation and characterisation of longibrachins LGA I and LGB II

Longibrachins LGA and LGB natural mixtures were isolated from cultures of *Trichoderma longibrachiatum* (strain LCP-853431, MNHN) by a multistep chromatography procedure involving exclusion chromatography (Sephadex LH20, MeOH as eluent), adsorption chromatography (SiO_2, CH_2Cl_2/MeOH 90/10 to 50/50) and semi-preparative reversed-phase HPLC. The HPLC separations were carried out either with a Waters (600E pump controller, 717 autosampler, 486 UV-vis. detector) or a Merck (L6200 intelligent pump, AS-200 autosampler, L4100 UV-vis. detector) liquid chromatograph. The separation conditions were: LGA I, Kromasil C18-5 μm, 7.5×300 mm (AIT France), MeOH/H_2O 85/15, $R_t=24$ min; LGB II: Spherisorb ODS2-5 μm, 7.5×300 mm (AIT France), MeOH/H_2O/TFA 84/14/0.05, $R_t=23.5$ min. The sequences of longibrachins LGA I and LGB II have been determined by mass spectrometry and two-dimensional NMR [24,25] and their helical conformation issued from NOE and CD data [25].

2.2. Peptide reconstitution into large area planar lipid bilayers

In macroscopic conductance experiments, virtually solvent-free lipid bilayers were formed over a 150–200 μm diameter hole in a 10-μm-thick Teflon film (Goodfellow, Cambridge, UK) sandwiched between two half glass cells. Lipid monolayers were spread on top of electrolyte solutions (1 M KCl, 10 mM HEPES, pH 7.4) in both compartments. Bilayer formation was most often achieved by lowering and then raising the level in one or both sides [26] and monitored by capacity responses. The lipid solution at 1–5 mg/ml in hexane was either a mixture: 1-palmitoyl, 2-oleoyl phosphatidylcholine (POPC)/1,2-dioleoyl phosphatidylethanolamine (DOPE), 7:3 (w/w), or diphytanoyl phosphatidylcholine (DPhPC). These lipids were purchased from Avanti Polar Lipids (Alabaster, AL, USA) and stored at −74°C. Voltage was applied through an Ag/AgCl electrode in the *cis*-compartment. Longibrachins were added from a stock solution in methanol (5×10^{-5} M). Transmembrane currents were fed to a Keithley amplifier (model 427, Cleveland, OH) virtually grounded to the *trans*-Ag/AgCl electrode. Current–voltage curves were recorded on an *X–Y* plotter (model LY1600, Linseis, Selb, Germany).

2.3. Single-channel recordings in Montal–Mueller type bilayers

The measurement cell was the same as described above. Single-channel currents were recorded using a BLM-120 amplifier (Bio-Logic, Claix, France). The fluctuations were filtered with an eight-pole Bessel filter AF-180 (Bio-Logic). Recordings were stored on a digital tape recorder DTR-1200 (Bio-Logic) and analysed with Satori vs. 3.01 software (Intracell, Royston, UK).

2.4. Single-channel recordings in bilayers made at the tip of patch-clamp pipettes

In 'tip-dip' experiments, lipid bilayers were formed at the tip of fire-polished patch-clamp pipettes pulled in two steps (model PP-83, Narishige, Tokyo, Japan) from GB150 glass capillaries (Bio-Logic). After this treatment, the tip diameter could be estimated to 0.5–1.0 μm and its resistance in the standard solution used for conductance measurements was of the order of 5 MΩ. The same lipid mixtures, as in the macroscopic conductance configuration but at 0.1–0.5 mg/ml in hexane, were allowed to evaporate on the top

of 2 ml of the electrolyte solution in a glass cell (2 cm diameter). To form bilayers, either the pipette was withdrawn and then slowly dipped again (by means of a hydraulic micro-manipulator, model 468M, L.S. Starrett, UK) or a lipid droplet was applied to the pipette shank [27]. Single-channel currents were recorded via a patch-clamp amplifier (RK-300, Bio-Logic) after filtering, on a digital tape recorder (respectively, AF 180 and DTR 1200 models from Bio-Logic).

For the analysis of single-channels temperature dependence, the temperature of the cell was monitored using a thermostat (model RM6, Lauda, Germany). A solution of DPhPC dissolved in hexane (1–5 mg/ml) was evaporated on the top of the bath solution before lowering the temperature. After 1 h, the test of bilayer formation was performed and single-channel currents were recorded after temperature measurement with a micro-tip thermometer (model 7001PL, JENCO, Taiwan).

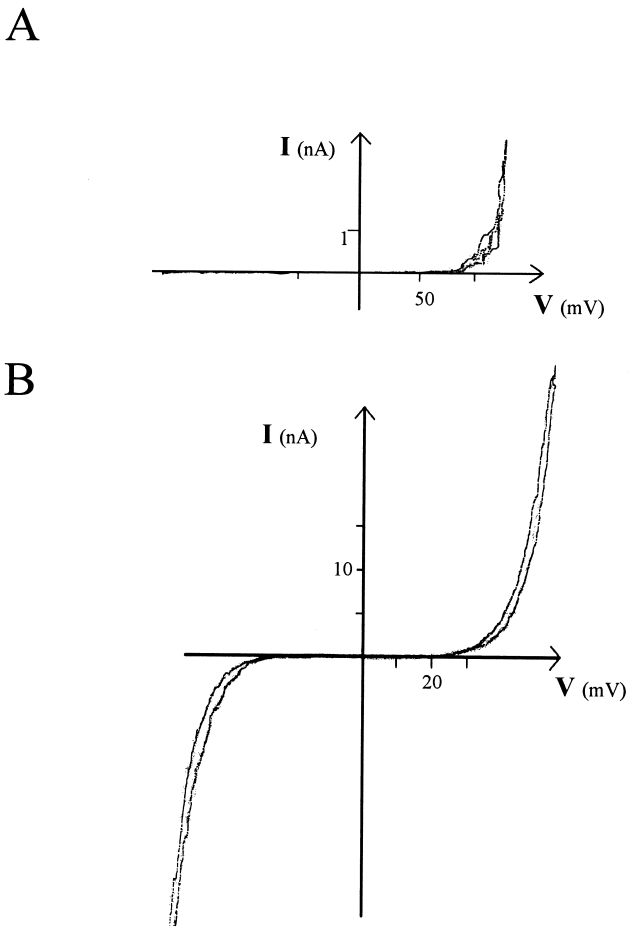

Fig. 1. Typical voltage-dependent *I–V* curves for longibrachin LGA I in Montal–Mueller type bilayers. (A) Curve recorded after asymmetrical addition of 3 μl of a 10 μM LGA I methanolic solution (bath final concentration: 15 nM) in only one compartment (*cis*-side) and after 1 h equilibrium. (B) Symmetrical curve obtained after addition of LGA I in both compartments (30 nM). In these conditions, similar V_c values (voltage threshold allowing to reach the reference conductance fixed to 50 nS) around 35–40 mV were found for the two branches. Lipids used were a 7:3 mixture of POPC/DOPE and the electrolyte solution was 1 M KCl, 10 mM HEPES (pH 7.4). The macroscopic current measurements were performed at room temperature and the *I–V* curves were recorded at a potential sweep rate of 10 mV/s.

3. Results

3.1. Macroscopic current measurements

Longibrachins LGA I and LGB II were incorporated into POPC/DOPE (7:3) planar lipid bilayers formed according to the Montal–Mueller technique. Both analogues induced typical alamethicin-like voltage-dependent macroscopic conductance (Fig. 1). The development of exponential branches occurred above a voltage threshold (V_c), which depended upon the peptide concentration in the bath. After addition of longibrachin LGA I or LGB II to only one compartment (*cis*-side), the bilayers were submitted to repetitive voltage-ramps. The first *I–V* plots could be recorded a few minutes after the peptide addition and a reproducible current level was reached after about half an hour, indicating that both longibrachins equilibrated rapidly between the bath and the bilayer. In these conditions, highly asymmetrical *I–V* curves were recorded and superimposed to ensure that partitioning equilibrium between peptide and membrane was reached (Fig. 1A). This asymmetry was observed for both the neutral (Gln-18) LGA I and the charged (Glu-18) LGB II. In the case of a symmetrical peptide addition, the symmetry of the *I–V* curves was recovered (Fig. 1B).

Macroscopic current measurements performed with different longibrachin concentrations allowed to estimate the concentration-dependence by measuring V_a, which is the shift of voltage threshold produced by an *e*-fold change in bath peptide concentration (Fig. 2). When selecting arbitrarily a V_c value

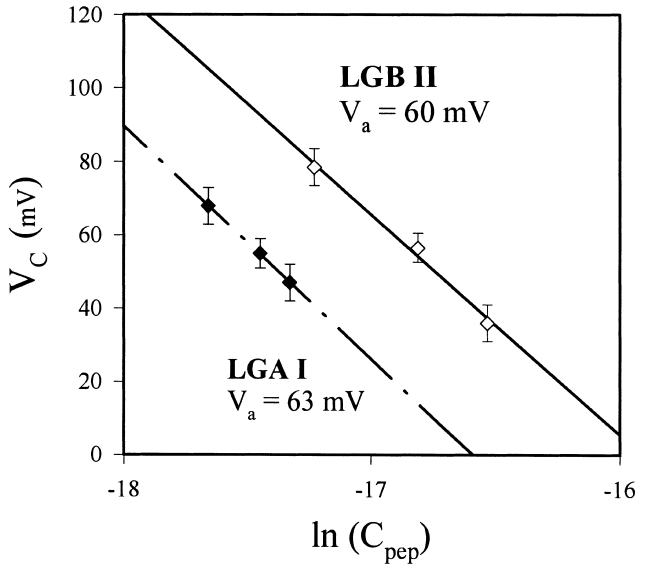

Fig. 2. Concentration dependence of macroscopic currents. Curves were obtained for LGA I and for LGB II in POPC/DOPE (7:3) bilayers bathed with 1 M KCl, 10 mM HEPES (pH 7.4). The evolution of V_c, the characteristic voltage threshold required to reach the 50 nS reference conductance is plotted as a function of Ln (bath peptide concentration). The slope ($-V_a$) reflects the voltage threshold shift resulting from an *e*-fold change in bath peptide concentration.

of 50 mV, a LGA I concentration of 28 nM was required to reach the 50 nS reference conductance, while this concentration was increased to 55 nM in the case of LGB II. This indicated a higher channel-forming activity of LGA I, reflecting a more pronounced affinity for the membrane bilayer, presumably due to its higher hydrophobicity. Moreover, a fast decrease in the V_c parameter as a function of the peptide concentration (Fig. 2) was indicative of a high concentration-dependence [22], since V_a values of 63 and 60 mV were determined for LGA I and LGB II, respectively. Finally, the voltage-increment resulting in an *e*-fold change in conductance, which is characteristic of the voltage-dependence, was identical for both longibrachins (V_e = 6 mV). As the V_a/V_e ratio allows to estimate an apparent mean number of monomers per conducting aggregate (n_{app}) [22], both longibrachins reflected a tendency to form large oligomers (n_{app} = 10 for LGA I and LGB II). The macroscopic current characteristics measured for longibrachins LGA I and LGB II appeared similar to those determined previously for Alm F30 I, [20,22,28] making them among the most efficient analogues of the peptaibol group, as regard their ability to induce large reversible currents in planar lipid bilayers.

3.2. Single-channel recordings

Typical single-channel current traces induced by longibrachins LGA I and LGB II (Fig. 3) indicated the multi-state behaviour already described for Alm and for related long-sequence peptaibols [21,28–30]. The concentration thresholds required to induce channel-forming activity remained similar to those determined in macroscopic current measurements. The traces presented for LGA I (Fig. 3A) and LGB II (Fig. 3B) were recorded at room temperature in POPC/DOPE bilayers using the Montal–Mueller technique, while those shown in Fig. 3C and D were performed in DPhPC bilayers at the tip of patch pipettes in order to resolve the faster transitions observed with this lipid. Indeed, in the POPC/DOPE mixture, mean open times for the different sublevels were in the range of 5–10 ms, whereas they were 1–2 ms in DPhPC bilayers (Table 2).

Although a large controversy subsists about the attribution of the lowest degree of association that forms a channel, the lower conductance level observed around 50 pS for both longibrachins should correspond to the smallest aggregate able to create a channel. The geometrical progression of the increments between the averaged conductance values (Table 2) was in agreement with the 'barrel-stave' model already proposed for Alm [13,14] and characterised by uptake and release of monomers in conducting bundles. The first O2 and O3 sublevel conductances observed in the two lipid compositions were practically similar for LGA I and LGB II. Nevertheless, above the O3 sublevel, the conductance values became higher in the case of LGB II. When comparing the conductance levels induced in POPC/DOPE bilayers, by Alm F30 I and LGB II which have both a glutamic acid at position 18, the three first O1, O2 and O3 levels were higher for Alm, whereas O4, O5 and O6 levels appeared quite similar for the two peptides.

The traces in Fig. 3 and the lifetime values of the substates (Table 2), allowed to follow the evolution of the conductance levels as a function of a virtual number of monomers. The data show that higher

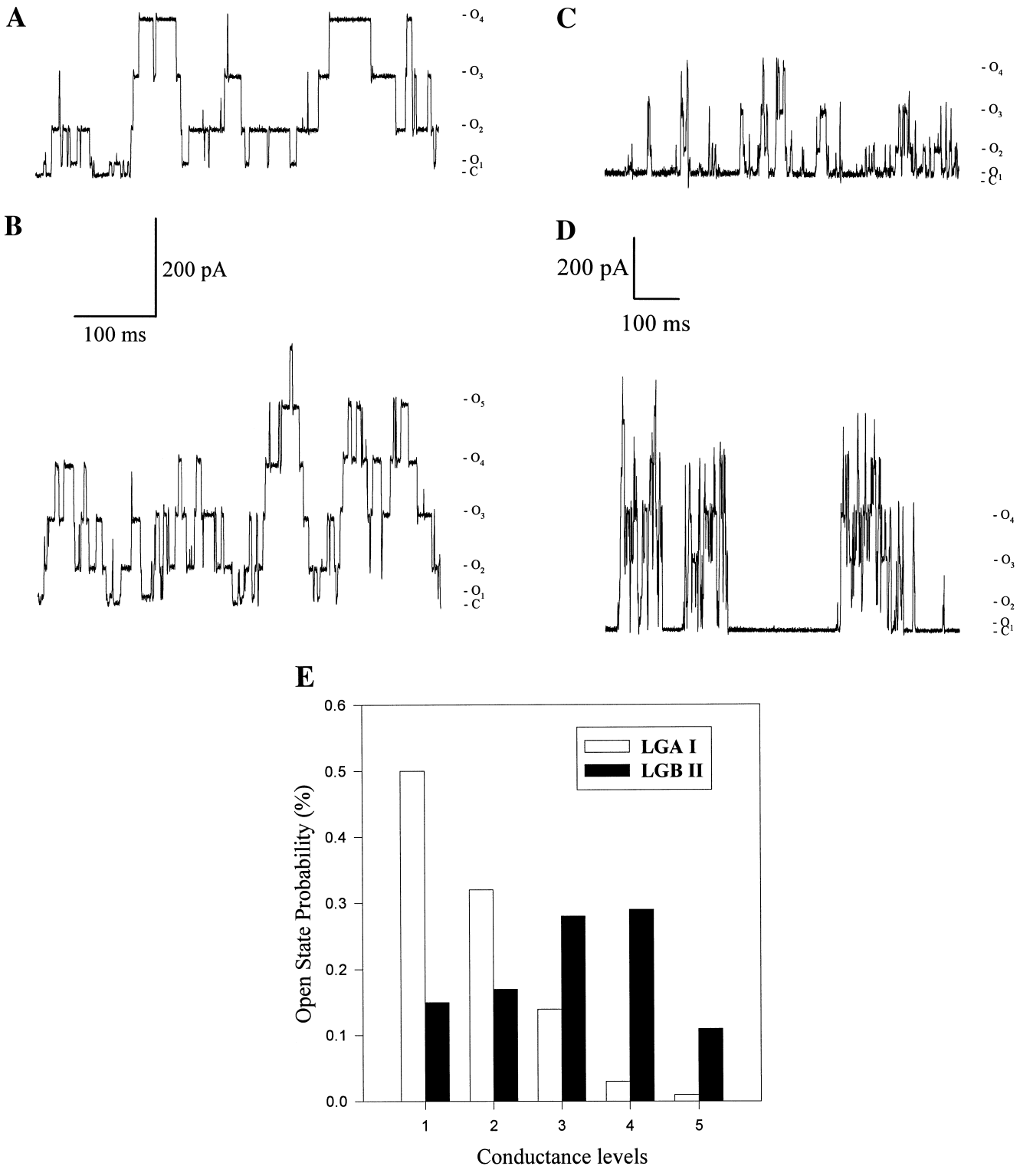
A
- O4
- O3
- O2
- O1
- C
C
- O4
- O3
- O2
- O1
- C
B
200 pA
100 ms
- O5
- O4
- O3
- O2
- O1
- C
D
200 pA
100 ms
- O4
- O3
- O2
- O1
- C
E
LGA I
LGB II
Open State Probability (%)
0.0
0.1
0.2
0.3
0.4
0.5
0.6
1
2
3
4
5
Conductance levels

Fig. 3. Single-channel recordings for longibrachins LGA I and LGB II. These currents were recorded after incorporation of the longibrachins either in POPC/DOPE (7:3) in Montal–Mueller bilayers (A, LGA I; B, LGB II; both at 100 mV) or in DPhPC bilayers formed at the tip of patch-clamp pipettes (C, LGA I; D, LGB II; both at 120 mV). Peptide concentrations were 15 nM for LGA I and 25 nM for LGB II. Electrolyte solutions were symmetrical 1 M KCl, 10 mM HEPES (pH 7.4). Bessel filter was set to 10 kHz during acquisition and the data were digitised at 25 kHz for computer analysis. (E) Compared open states probabilities for the first five conductance levels in DPhPC bilayers. The histogram was drawn from the single-channel recordings displayed in C and D. The closed state was not taken into account and the sum of the open states probabilities was normalised to 100%. The probabilities of the closed states were 0.55 and 0.85 for LGA I and LGB II, respectively.
←

sublevels were favoured in the case of the charged longibrachin LGB II, specially in DPhPC bilayers (Fig. 3E) and that the channel lifetimes were about two times longer for LGA I, whatever the bilayer composition. Moreover, the lifetimes of all the sublevels were higher for Alm compared to LGB II.

In order to analyse the evolution of the channel stability as a function of the temperature, several assays were performed in the range 7–25°C, with the neutral longibrachin LGA I incorporated into DPhPC bilayers using the 'tip–dip' set-up. Fig. 4 shows the evolution of single-channel fluctuations observed at three temperatures with a constant peptide concentration of 50 nM. We first observed that the potential necessary to induce single channels had to be increased according to the temperature decrease. Indeed, if a single-channel activity could be recorded at a potential about 30–50 mV at 25°C, a value of 100–150 mV was required at 12°C. This observation argued for a markedly reduced voltage-dependence at lower temperatures. Moreover, the increase of channel lifetimes was observed with the temperature decrease (Table 3), a ratio of 3 for an 11°C decrease being noticed. For instance, the third open level had a mean open time of 4 ms at 18°C and of 12 ms at 7°C. Finally, we also observed a decrease of the conductance values with decreasing the tem-

Table 2
Conductance levels and substate lifetimes for longibrachins LGA I and LGB II (in 1 M KCl, 10 mM HEPES, pH 7.4) and for Alm F30 I[a]

			O1	O2	O3	O4	O5	O6
LGAI	γ (pS)	A	40	265	1025	2175	3410	4735
		B	n.d.	140	815	2040	3390	n.d.
	τ (ms)	A	n.d.	5.0	7.5	10.4	10.3	6.7
		B	n.d.	1.6	2.0	2.1	1.8	n.d.
LGBII	γ (pS)	A	70	215	935	2425	3975	5620
		B	n.d.	200	925	2320	3845	5340
	τ (ms)	A	n.d.	2.2	3.7	5.7	6.5	4.4
		B	n.d.	1.0	1.1	1.4	1.7	1.3
Alm F30I	γ (pS)	A	170	400	1300	2500	4000	5600
	τ (ms)	A	10	34	59	96	71	45

Data from Bienert et al. [20,29]. A, POPC/DOPE (7:3) mixture; B, DPhPC.

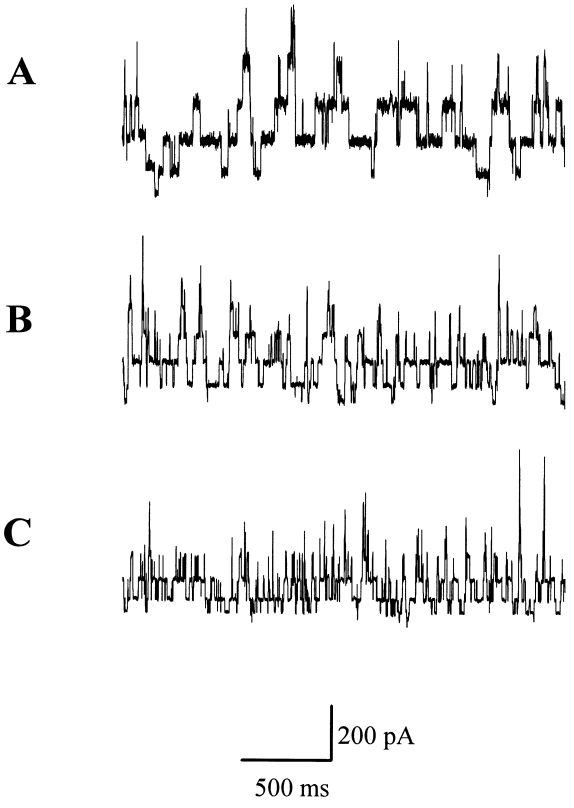

Fig. 4. Single-channel currents induced by LGA I at different temperatures. These fluctuations were recorded with a constant peptide concentration 50 nM in DPhPC bilayers made at the tip of patch pipettes. Electrolyte solution was 1 M KCl, 10 mM HEPES (pH 7.4). Experimental conditions: A, $T=7$°C, $V=155$ mV; B, $T=12$°C, $V=130$ mV; C, $T=18$°C, $V=90$ mV.

Table 3
Mean open times as a function of temperature for LGAI

	7°C	12°C	18°C
τ_{O1} (ms)	8.0	4.7	2.9
τ_{O2} (ms)	11.2	7.6	5.0
τ_{O3} (ms)	12.1	8.5	4.5
τ_{O4} (ms)	6.6	4.3	3.2
τ_{O5} (ms)	3.0	2.3	1.0
γ_{O1} (nS)	0.19	0.25	0.21
γ_{O2} (nS)	0.51	0.67	0.73
γ_{O3} (nS)	1.00	1.29	1.55
γ_{O4} (nS)	1.60	1.94	2.51
γ_{O5} (nS)	2.25	2.69	3.60

Single-channel currents were recorded in DPhPC bilayers formed at the tip of patch pipettes bathed with 1 M KCl, 10 mM HEPES (pH 7.4). τ_{Oi} values are the mean open times and γ_{Oi} values are the conductances levels for the five first states.

perature: these values were 0.73 and 3.60 nS for the second and fifth open states at 18°C, respectively, while they decreased to 0.51 and 2.25 nS at 7°C. These results are in agreement with the recent observation that 18-residue neutral peptaibols which only result in fast current fluctuations which cannot be resolved at room temperature, recover the characteristic multi-state behaviour of the prototypic Alm, if the temperature is decreased to 10°C [8].

4. Discussion

According to electrophysiological studies (reviewed by Sansom [10]) and to the generally admitted 'barrel-stave' channel model of alamethicin, the peptide N-terminus should be inserted deeply in the bilayer, while the C-terminus should act as an anchor at the *cis*-bilayer surface. In this model, the Gln-7, Gly-11, Pro-14 and Glu-18 amino acids are directed toward the water-filled channel interior, while the Pro-2 residue is involved in the peptide/peptide interactions, and thus in the bundle stabilisation. The channel lining thus consists in polar rings occurring at different levels of the helix bundles. In the present work, we have characterised the channel-forming activity of longibrachins LGA I and LGB II, the 20-residue peptaibols which differ between them by a Gln-18/Glu replacement and distinguish by the single Pro-2/Ala substitution from alamethicins F50 (Alm F50) and F30 I (Alm F30I), respectively. These amino acid substitutions in the Alm sequence should allow to estimate the role and function in the ion-channel activity of the critical residues Pro-2 and Glu-18 located at the very N- and C-termini of the peptide.

We have shown that none of the two examined substitutions in the Alm primary structure alters the voltage activity of the ion-channel. In planar lipid bilayers, both longibrachins exhibit macroscopic and single-channel activities similar to those described for Alm and related analogues [2,9,21,28–31]. As previously observed for charged and neutral 20-residue peptaibols, such as Alm and its synthetic analogues [19,20,29] trichosporin [30] and trichocellins [21], longibrachins LGA I and LGB II both result in asymmetrical macroscopic conductance curves, when the peptide is added to the *cis*-side. Thus, the hypothesis consisting of a possible reorientation of dipoles after statistical orientation [31,32] is not privileged. In such a model, channels should activate at both polarities in respect to their statistical orientation. Our results indicate that the long-sequence peptaibols orient specifically and that their propensity to flip-flop is rather limited. They are in agreement with recent molecular dynamic simulations of Alm in POPC bilayers [33] which suggest that the asymmetrical insertion of the Alm helices is related to the pair of polar side chains at positions 18 and 19 which constitute the basis of the C-terminal anchor at the bilayer surface. Such an Alm/water interaction does not occur at the N-terminus, resulting in the observed asymmetry.

When comparing the characteristic values of voltage-dependence, a similar V_e value of around 6 mV is observed for Alm F30 I (Pro-2, Glu-18) and for longibrachins LGB II (Ala-2, Glu-18) and LGA I (Ala-2, Gln-18). Similar V_e values for both neutral and charged analogues have been also reported for related analogues [21], and do not argue for the hypothesis in which the peptides move parallel to the membrane field from a partially external position during voltage-dependent activation [4]. From the present results, the voltage-dependent process would rather implicate a rocking motion associated with a translation in the membrane plane for which the Glu-18 motion would be very small. Moreover, the

same concentration-dependence is noticed for the two longibrachins and for Alm F30 I, for which the same mean number of monomers ($n_{app} = 10$) involved in channel formation has been determined. The above characteristics identify alamethicins and longibrachins as the most efficient peptaibols with respect to their ability to induce high ionic currents in membranes. The n_{app} values appear lower in the case of the previously studied saturnisporin SAIV ($n_{app} = 6$) [7], trichocellins ($n_{app} = 6$) [21] and trichosporin TSB VIa ($n_{app} = 7$) [30]. However, the observed macroscopic behaviour changes result from several substitutions in the Alm sequence in addition to the Pro-2/Xaa one (Table 1). Our results clearly show that the Pro-2/Xaa substitution is without noticeable effect on the macroscopic current parameters and thus indicate that the decrease in n_{app} observed with these analogues is rather due to the other amino acid substitutions at positions 6, 9 and 12. These positions are occupied by sterically hindered amino acids which are located in regions of the peptide which may play an important role in the interaction between the peptide helices and the hydrophobic core of the bilayer.

The results of the single-channel experiments confirm at the molecular level the similar behaviour observed at the macroscopic level for longibrachins and alamethicins. Indeed, the conductance values of the substates are very similar among the neutral and charged peptides [20,34]. The Pro-2/Ala and Glu-18/Gln substitutions in these peptaibols do not appear to change drastically the channel size of the conducting bundles. As regard the channel stability, higher degrees of oligomerisation are favoured in the case of the charged longibrachin LGB II, as shown by the larger open state probabilities and increased mean dwell-times observed for the higher substates. Indeed, the Glu/Gln residue at position 18 has its side chain projected in the hydrophilic sector of the helix and is oriented inside the channel. Thus, a repulsive effect seems to arise between the charged longibrachin monomers, presumably because of the presence of too nearby negative charges. The high occurrence of large size channels with this charged peptaibol is certainly a direct consequence of the electrostatic repulsion which tends to put away monomers and to favour additional monomer insertion. In the case of the charged trichocellin [21], a very similar pattern has been also described, supporting the idea of electrostatic repulsion occurring in small size aggregates.

Most interesting is the reduction of substate lifetimes induced by the Pro-2/Ala replacement. This finding, closely similar to that already observed with the Des-Aib-Leu synthetic analogues [19], points to a weaker stabilisation of the channels formed by peptaibols lacking a proline at the N-terminus. This point suggests a particular role of Pro-2 in the stabilisation of the conducting bundles. Given the higher hydrophobicity of Ala compared to Pro [35–38], the reduced substate lifetimes could reflect a less efficient anchoring at the *trans*-hydrophobic core/lipid head interface of the peptaibol N-terminus lacking the proline, unless specific steric hindrance effects have to be considered.

Finally, examination of the role of temperature on the channel-forming properties showed a decrease of the voltage-dependence with the decrease in temperature. Indeed, single-channel activity can be detected in an enlarged range of potential at lower temperatures. Moreover, a decrease of temperature also creates a pronounced channel lifetime increase. The lateral diffusion of lipids is greatly reduced with the temperature decrease [39], the channel activity being thus significantly modified. That contributes to delay the diffusion of an embedded monomer in a conducting aggregate, increasing notably the substate lifetimes. It would be of interest to check this result and quantify the voltage- and concentration-dependencies as a function of temperature at the macroscopic current level, as such an effect of the temperature is of particular interest to resolve and analyse the very fast current fluctuations induced by shorter peptides in standard conditions [8].

In conclusion, this study confirms the strong stabilisation of the channels afforded by a Glu residue at the C-terminus of the peptide helix, that acts as an anchor at the *cis*-bilayer/water interface and supports the idea that Pro-2 at the N-terminus provides additional stabilisation at the *trans*-bilayer interface. However, the main characteristics of ion-channel activity responding to the 'barrel-stave' mechanism remain unmodified by the Glu-18/Gln and Pro-2/Ala substitutions occurring in the natural peptaibols, while other substitutions which have been realised with synthetic peptides have resulted in stronger

modifications of the conductance properties. This fact points to the optimal activity acquired by the natural peptaibols through evolution, as regard their voltage-gated membrane properties.

Acknowledgements

P. Cosette greatly thanks a postdoctoral funding accorded by the 'Conseil Régional de Haute-Normandie'. This work was supported by a CNRS grant from the GDR 790.

References

[1] C.E. Meyer, F. Reusser, Experientia 23 (1967) 85–86.
[2] L.G.M. Gordon, D.A. Haydon, Biochim. Biophys. Acta 255 (1972) 1014–1018.
[3] R.C. Pandey, J.C. Cook, K.L. Rinehart, J. Am. Chem. Soc. 99 (1977) 8469–8483.
[4] F.O. Fox, F.M. Richards, Nature 300 (1982) 325–330.
[5] I.L. Karle, P. Balaram, Biochemistry 29 (1992) 6747–6756.
[6] M. El Hajji, S. Rebuffat, T. Le Doan, G. Klein, M. Satre, B. Bodo, Biochim. Biophys. Acta 978 (1989) 97–104.
[7] S. Rebuffat, H. Duclohier, C. Auvin-Guette, G. Molle, G. Spach, B. Bodo, FEMS 105 (1992) 151–160.
[8] D. Duval, P. Cosette, S. Rebuffat, H. Duclohier, B. Bodo, G. Molle, Biochim. Biophys. Acta 1369 (1998) 309–319.
[9] S. Rebuffat, G. Goulard, B. Bodo, M.-F. Roquebert, The peptaibol antibiotics from Trichoderma soil fungi; structural diversity and membrane properties. Recent Developments in Organic and Bioorganic Chemistry, Transworld Research Network, Trivandrum, India, in press.
[10] R. Latorre, O. Alvarez, Physiol. Rev. 61 (1981) 77–150.
[11] M.S.P. Sansom, Q. Rev. Biophys. 26 (1993) 365–421.
[12] L. Béven, D. Duval, S. Rebuffat, F.G. Riddell, B. Bodo, H. Wroblewski, Biochim. Biophys. Acta 1372 (1998) 78–90.
[13] G. Bauman, P. Mueller, J. Supramol. Struct. 2 (1974) 538–557.
[14] G. Boheim, J. Membr. Biol. 19 (1974) 277–303.
[15] D.N. Woolfson, D.H. Williams, FEBS Lett. 277 (1990) 185–188.
[16] L. Piela, G. Nemethy, H.A. Scheraga, Biopolymers 26 (1987) 1587–1600.
[17] F.G. Franklin, J.F. Ellena, S. Jayasinghe, L.P. Kelsh, D.S. Cafiso, Biochemistry 33 (1994) 4036–4045.
[18] E. Condamine, S. Rebuffat, Y. Prigent, I. Ségalas, B. Bodo, D. Davoust, Biopolymers 46 (1998) 75–88.
[19] H. Duclohier, G. Molle, J.-Y. Dugast, G. Spach, Biophys. J. 63 (1992) 868–873.
[20] C. Kaduk, H. Duclohier, M. Dathe, H. Wenschuh, M. Beyermann, G. Molle, M. Bienert, Biophys. J. 72 (1997) 2151–2159.
[21] S. Wada, A. Iida, K. Asami, E. Tachikawa, T. Fujita, Biochim. Biophys. Acta 1325 (1997) 209–214.
[22] I. Vodyanoy, J. Hall, T.M. Balasubramniam, G.R. Marshall, Biochim. Biophys. Acta 684 (1982) 53–58.
[23] N. Koide, K. Asami, T. Fujita, Biochim. Biophys. Acta 1326 (1997) 47–53.
[24] G. Leclerc, S. Rebuffat, C. Goulard, B. Bodo, J. Antibiot. 51 (1998) 170–177.
[25] S. Hlimi, Ph.D. Thesis, University P. and M. Curie, Paris, France, 1997.
[26] M. Montal, P. Mueller, Proc. Natl. Acad. Sci. USA 69 (1972) 3561–3566.
[27] W. Hanke, C. Methfessel, W. Wilmsen, G. Boheim, Bioelectrochem. Bioenerg. 12 (1984) 329–339.
[28] L.G.M. Gordon, D.A. Haydon, Philos. Trans. R. Soc. Lond. Ser. B 270 (1975) 433–447.
[29] C. Kaduk, M. Dathe, M. Bienert, Biochim. Biophys. Acta 1373 (1998) 137–146.
[30] Y. Nagaoka, A. Iida, T. Kambara, K. Asami, E. Tachikawa, T. Fujita, Biochim. Biophys. Acta 1283 (1996) 31–36.
[31] G. Boheim, W. Hanke, G. Jung, Biophys. Struct. Mech. 9 (1983) 181–191.
[32] M.K. Mathew, P. Balaram, FEBS Lett. 157 (1983) 1–5.
[33] D.P. Tieleman, M.S.P. Sansom, H.J.C. Berendsen, Biophys. J. 76 (1999) 40–49.
[34] O. Helluin, J.-Y. Dugast, G. Molle, A.R. Mackie, S. Ladha, H. Duclohier, Biochim. Biophys. Acta 1330 (1997) 284–292.
[35] J. Kyte, R.F. Doolittle, J. Mol. Biol. 157 (1982) 105–132.
[36] D. Eisenberg, E. Schwarz, M. Komaromy, R. Wall, J. Mol. Biol. 179 (1984) 125–142.
[37] P.R. Gibbs, A. Radzicka, R. Wolfenden, J. Am. Chem. Soc. 113 (1991) 4714–4715.
[38] T.E. Thorgeirsson, C.J. Russell, D.S. King, Y.-K. Shin, Biochemistry 35 (1996) 1803–1809.
[39] M.D. King, D. Marsh, Biochim. Biophys. Acta 862 (1986) 231–234.